

Open Access Article

The Effect of Peroxide on the Film Blowing Stability and Rheological Properties of Polylactic acid Blown Films

Peerapong Chanthot¹, Noppadon Kerddonfag², Cattaleeya Pattamaprom¹

¹ Research Unit in Polymer Rheology and Processing, Department of Chemical Engineering, Faculty of Engineering, Thammasat University, Pathum Thani 12120, Thailand

² National Metal and Materials Technology Center, National Science and Technology Development Agency, Thailand Science Park, Pathum Thani 12120, Thailand

Abstract: This study is the first study correlating the effect of the peroxide branching agent with the film blowing stability of polylactic acid (PLA). The peroxide content was varied between 0-0.5 wt%, and the changes in molecular structures, rheological properties, film bubble stability, and mechanical properties were investigated. Our research goal is to improve the processability of PLA blown film and identify key parameters for the good processability of PLA. It was found that the addition of a sufficiently high peroxide content led not only to higher storage modulus (G') but also to higher melt strength and significant improvement in the film blowing processability, where the blow-up ratio (BUR) increased with increasing peroxide content. However, the peroxide content higher than 0.3 wt% tended to cause stiffer film and a higher amount of gels. Another interesting finding is that the terminal region's G value was strongly correlated with melt strength and film blowing processability.

Keywords: polylactic acid, film blowing, peroxide, processability, rheological properties.

过氧化物对聚乳酸吹膜稳定性和流变性能的影响

摘要:

该研究是首次将过氧化物支化剂的影响与聚乳酸的吹膜稳定性相关联的研究。过氧化物含量在0-0.5重量-重量%之间变化,并研究了分子结构、流变性能、薄膜气泡稳定性和机械性能的变化。我们的研究目标是提高聚乳酸吹膜的加工性能,并确定聚乳酸良好加工性能的关键参数。发现添加足够高的过氧化物含量不仅导致更高的储能模量(G'),而且导致更高的熔体强度和薄膜吹塑加工性的显著改善,其中吹胀比(伯尔)随增加过氧化物含量。然而,高于0.3重量-重量%的过氧化物含量往往会导致更硬的薄膜和更多的凝胶量。另一个有趣的发现是末端区域的 G 值与熔体强度和吹膜加工性密切相关。

关键词: 聚乳酸, 吹膜, 过氧化物, 加工性, 流变特性。

1. Introduction

Nowadays, plastic waste from fossil-based non-degradable plastic has caused serious environmental concerns, and more attention is being paid to biodegradable plastics. Polylactic acid (PLA) is one of the biobased and biodegradable plastics in the group of

thermoplastic polyester [1], [2]. PLA has become an interesting plastic for green packaging and biomedical applications because of its biocompatibility, high strength, and transparency [3]. However, PLA has posed several challenges, especially in the extrusion

Received: May 26, 2021 / Revised: June 6, 2021 / Accepted: July 23, 2021 / Published: August 30, 2021

About the authors: Peerapong Chanthot, Research Unit in Polymer Rheology and Processing, Department of Chemical Engineering, Faculty of Engineering, Thammasat University, Pathum Thani, Thailand; Noppadon Kerddonfag, National Metal and Materials Technology Center, National Science and Technology Development Agency, Thailand Science Park, Pathum Thani, Thailand; Cattaleeya Pattamaprom, Research Unit in Polymer Rheology and Processing, Department of Chemical Engineering, Faculty of Engineering, Thammasat University, Pathum Thani, Thailand

film blowing process. These include very poor film blowing processability (poor bubble instability) [4], [5].

To improve the film blowing processability of PLA, Karkhanis et al. [5] reported processability improvement by adjusting the process parameters, including the reduction in melt temperature and the adjustment of internal and external air pressures. In addition, chain extenders such as multifunctional epoxies, PDLA-g-PEG-g-PDLA triblock polymer, and methyl methacrylate/glycidyl methacrylate copolymer are often blended with PLA to increase its melt strength [6], [7], [8], [9], [10]. Among these, only one research paper was relevant to film blowing of neat PLA. Lamnawar et al. [7] found that Joncryl[®] ADR-4368, a commercial multifunctional epoxide reactive polymer, could increase the elongational viscosity and blow-up ratio of PLA blown film.

Another interesting strategy to improve the properties of PLA is by reactive blending with peroxide. Göttermann et al. [11] reported that 0.2 wt% peroxides could increase the melt strength from 0.025 to 0.09 N, which was more than a threefold increase. Moreover, Hwang et al. [12] found that an increase in peroxide content (up to 0.8 wt%) could significantly increase the storage modulus (G') and complex viscosity (η^*) of PLA, where an optimal amount of peroxide could also slightly increase its impact strength and tensile properties. Even though these studies reported on the potential of peroxide in improving the melt strength and rheological properties of PLA, there is no study focusing on the processability improvement of PLA blown films. Therefore, this study aimed to investigate the effect of peroxide on the change in chemical structures and its consequence on rheological properties, bubble stability during film blowing, and mechanical properties of PLA.

2. Experiment

2.1. Materials

This study purchased PLA grade 4043D with the melt flow index (MFI) and the specific gravity of 6.0 g/10 minutes and 1.24 g/cc, respectively, from NatureWorks LLC, USA. Tert-butyl peroxide, an organic peroxide, was purchased from Sigma-Aldrich Co., Ltd, USA.

2.2. Reactive Melt Blending of PLA with Peroxide

First, PLA was dried overnight in a vacuum oven at 80 °C before blending with the organic peroxide in an internal mixer (Brabender Plasti-Corder[®] Lab-Station 350E, Germany). The blending was carried out for 15 minutes at 160 °C, and the rotor speed was 60 rpm. The code names of the peroxide-treated PLA samples were represented by PL_x, where x is the wt% of the organic peroxide. Here, the peroxide content was varied from 0, 0.003, 0.03, 0.1, 0.3 to 0.5 wt%, respectively.

2.3. Film Blowing Process

The peroxide-treated PLAs were cut into small granules by a granulator and dried overnight in a vacuum oven at 80°C to remove excess moisture. The compound was then blown into the film using a film blowing machine (HAAKE Rheomex OS, USA) at a fixed screw speed of 40 rpm and a processing temperature of 170-195 °C (4 zones). The schematic of a film blowing process is illustrated in Figure 1.

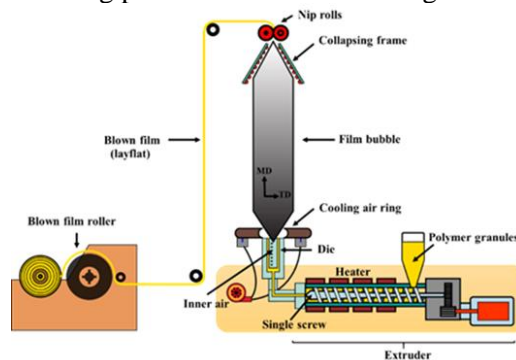


Fig. 1 The schematic of the film blowing process

2.4. Characterization

2.4.1. Fourier Transform Infrared Spectroscopy (FTIR)

Fourier transform infrared spectra of dried specimens were recorded using Fourier Transform Infrared Spectrometer (Perkin Elmer Spectrum[™] 3 FT-IR spectrometer, USA) equipped with universal attenuated total reflectance (UATR). The spectra were recorded between the wavenumber of 4,000 and 400 cm^{-1} .

2.4.2. Nuclear Magnetic Resonance Spectroscopy (NMR)

The unmodified PLA and peroxide-treated PLA were dissolved in deuterated chloroform (CDCl_3) at a concentration of 4 wt% at room temperature. ¹H-NMR spectra were recorded in the chemical shifts of 0-12 ppm using a 600 MHz NMR spectrometer (Ascend[™]600/Avance III HD, Bruker, USA).

2.4.3. Rheological Characterization

Before rheological measurement, the specimens were dried overnight in a vacuum oven at 80 °C, then prepared into discs of 25-mm diameter by compression molding at 190 °C for 3 minutes. The dynamic rheological properties of samples were measured at 170 °C using a modular compact rheometer (MCR102) equipped with a 25-mm parallel plate geometry from Anton Paar Ltd, Thailand. The gap was set at 0.5 mm. The strain amplitude sweep tests were carried out at the highest angular frequency to identify the linear viscoelastic region. The frequency sweep tests were carried out within the linear viscoelastic limit.

2.4.4. Melt Strength Measurement

Melt strength was measured using a capillary rheometer equipped with a melt strength tester (Rosand

RH7, Malvern, UK). The extrusion melt temperature was set at 190 °C. The polymer melt was extruded vertically from the capillary rheometer at a 100 mm/min extrusion rate. After the flow of extruded strand reached a steady state, the strand was drawn downwards uniaxially by the melt strength tester, which was composed of two counter-rotating steel rollers connected to a force transducer. The drawdown distance (from dying exit to rollers) was 15 cm. The speed of rollers increased at a constant acceleration rate (2.33 m/s^2) over a range from 10 to 800 m/min until the polymer melt strand was broken. The force at which the polymer melt broke was recorded as the melt strength.

2.4.5. Film Blowing Processability

Key parameters for the processability of a film blowing process are the blow-up ratio (BUR) and the take-up ratio (TUR). BUR refers to the ratio of the bubble diameter to the extrusion die diameter, and TUR refers to the ratio of take-up roller speed to the speed of the extruder's screw, as shown in the following equations [5].

$$\text{TUR} = (\text{Speed of take-up rollers}) / (\text{Speed of extruder's screw}) \quad (1)$$

$$\text{BUR} = (\text{Final bubble diameter}) / (\text{Die diameter}) \quad (2)$$

The screw speed of the extruder was calculated from $\pi DN/60$, where D is the diameter of the screw, and N is the rotational speed in rpm. In this work, N was fixed at 40 rpm, while the take-up speed of the nip rollers was varied. The bubble diameter was controlled by the flow rate of inner bubble air.

The processability of the film blowing process was considered from the highest blow-up ratio (BUR) at each take-up ratio (TUR). The correlations between TUR and the corresponding highest BUR were plotted on a stable bubble chart (BUR-TUR chart). The point of the highest BUR was indicated by the process condition that provided the highest bubble diameter without bubble dancing, melt sagging, or draw resonance for at least 3 minutes.

2.4.6. Film Thickness Uniformity

The film thickness uniformity is defined in terms of the uniformity index following equation 3. All blown film samples were measured for their thickness at 50 different positions at a distance of 5 cm apart along the machine direction. Higher uniformity index indicates a more stable film blowing process. The measurements were carried out on the film produced from a fixed TUR of 1.13.

$$\text{Uniformity index} = (\text{Average film thickness}) / (\text{Standard deviation}) \quad (3)$$

2.4.7. Tensile Testing

Tensile testing of PLA blown films was carried out according to ASTM D882 at ambient temperature by a Universal Testing Machine (UTM) model UTB9251-

ACHiTech from Narin Instruments, Thailand. The film samples with a size of 10 mm wide and 200 mm long were subjected to stress-strain measurement in the machine directions using a 0.98-kN load cell at the cross-head speed and gauge length of 20 mm/min and 100 mm, respectively. Five specimens were tested for each sample. The Young's modulus, tensile strength, elongation at break, and tensile toughness were calculated for each sample.

2.4.8. Gel Content

The peroxide-treated PLA compounds were ground into small pieces before immersing in acetone in the dark for 4 days at room temperature with periodic stirring to remove free PLA. The undissolved portions were then filtered out to isolate the insoluble components. The following equation calculated the gel content of a compound.

$$\% \text{ gel content} = (\text{Weight of insoluble portion}) / (\text{Weight of compound}) \cdot 100 \quad (4)$$

3. Results and Discussion

3.1. Characteristics of Peroxide-treated PLAs

In this study, the effects of peroxide on rheological properties and processability of PLA blown films were investigated at the peroxide contents of 0.003 to 0.5 wt%. The possible reaction mechanisms initiated by peroxide are illustrated in Figure 2. After the peroxide was thermally decomposed into peroxide radicals, these radicals then abstracted hydrogen from the PLA backbone leading to the generation of PLA radicals (Figure 2(a)). The termination of PLA radicals could happen in two pathways. One is by chain scission (Figure 2(b)) [13], [14]. This reaction was reported to happen at low peroxide contents [15]. The other is by recombination of PLA radicals leading to chain extension and branching (Figure 2(c)) [16].

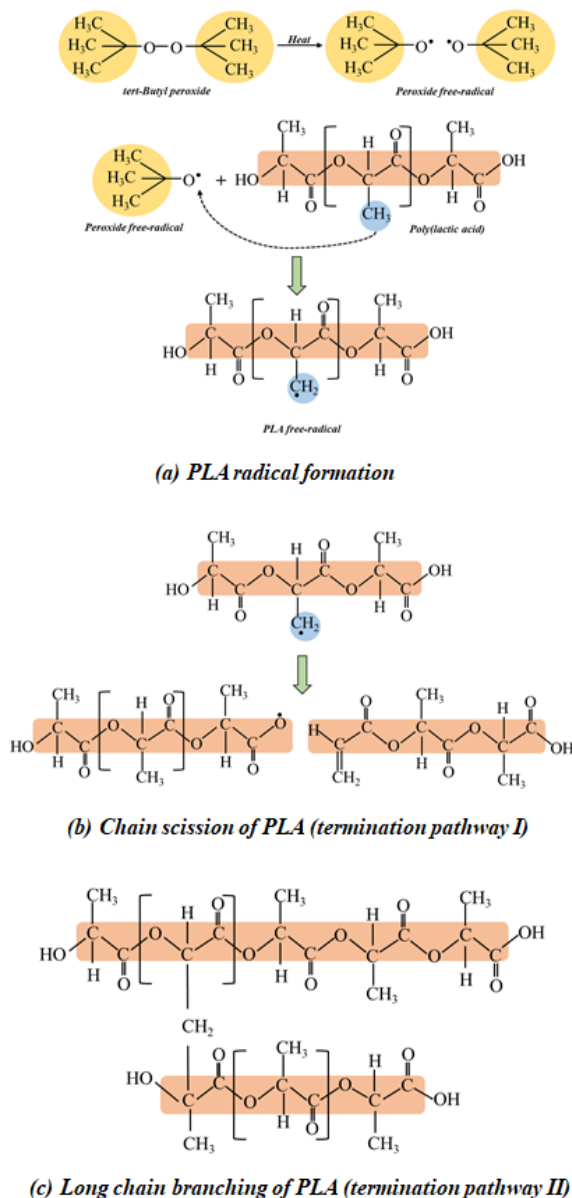


Fig. 2 The possible mechanisms for the reaction of peroxide with PLA

The FTIR spectra of untreated and peroxide-treated PLAs at 0.03 and 0.5 wt% are shown in Figure 3 to identify the changes in the molecular structure after peroxide treatment. The fingerprint of PLA showed the strong peaks of -C=O , -C-O , and C-O-C at 1747 cm^{-1} , 1180 cm^{-1} , and 1079 cm^{-1} , respectively. The double peaks at 2995 and 2945 cm^{-1} were assigned to symmetric and asymmetric stretching of -C-H from -CH_3 ; the weak peaks at 1127 cm^{-1} , 1043 cm^{-1} , and 867 cm^{-1} were assigned to the rocking of -CH_3 , stretching of -C-CH_3 stretching, and stretching of C-COO , respectively [13], [17], [18]. Unfortunately, after peroxide treatment at 0.03 wt% and 0.5 wt% (PL0.03 and PL0.5), the FTIR spectra did not change significantly from untreated PLA (see Table 1). It is probably because this method is not sensitive enough for small changes in the chemical structures.

Another approach to identifying the changes in chemical structure is by using the NMR technique. The $^1\text{H-NMR}$ spectra of the neat PLA and peroxide-treated

PLA samples are shown in Figure 4. As can be seen, the spectrum of neat PLA indicated sharp peaks at 5.19 and 1.59 ppm corresponding to the peaks of methine proton (C-CH) (peak (a)) and methyl proton (C-CH_3) (peak (b)), respectively. The spectrum of peroxide-treated PLA (PL0.03 and PL0.5) illustrated a slight increase in the peak heights of 4.39 and 2.51 ppm compared to PL0. These peaks correspond to the peaks of terminal methine protons at the chain ends, HC-OH (peak (d)) and HC-COOH (peak (e)), respectively. The increase in end groups could be evidence for peroxide-induced chain scission as proposed in Figure 2(b). The spectrum of PLA treated with 0.5 wt% peroxide (PL0.5) also indicated a significantly higher intensity of methylene proton (C-CH_2) (peak (c)) at 2.19 ppm than those of PL0 and PL0.03. It indicated that 0.5 wt% peroxides could promote the chain combination of PLA molecules, as proposed in Figure 2(c).

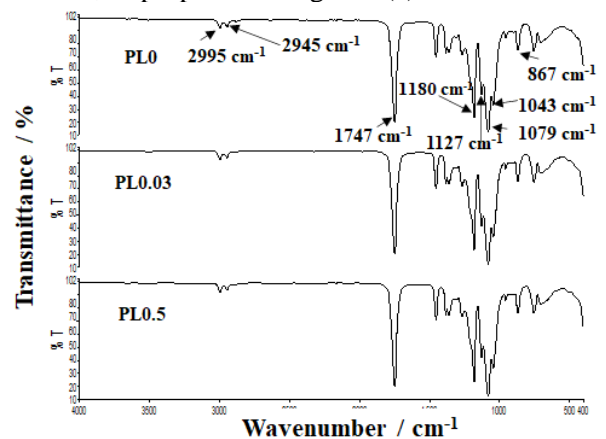


Fig. 3 FTIR (UATR) spectra of PLA and peroxide-treated PLAs using the peroxide content of 0.03 and 0.5 wt%

Table 1 FTIR absorbance peak height ratio of PLA and peroxide-treated PLAs

Sample	Height of -C-COO (A_{867}/A_{1747})	Height of C-O-C (A_{1079}/A_{1747})	Height of -CH_3 (A_{1127}/A_{1747})	Height of -C-CH_3 (A_{1043}/A_{1747})
PL0	0.21	0.40	0.24	0.23
PL0.03	0.21	0.40	0.24	0.23
PL0.5	0.21	0.41	0.23	0.23

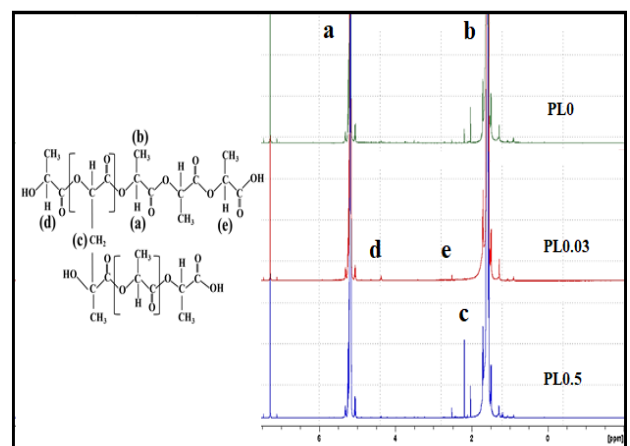


Fig. 4 $^1\text{H-NMR}$ spectra of PLA and peroxide-treated PLAs using peroxide contents of 0.03 and 0.5 wt%

The peroxide-initiated reaction that occurred during reactive melt blending was investigated in an internal mixer from the torque evolution, as shown in Figure 5. As can be seen, the initial increase in torque of all compounds during the first period (1-2 minutes) was due to the melting and mashing of the PLA pellets within the chamber. For the blends using high peroxide contents (0.1-0.5wt%), the second torque overshoot was observed in the blends at around 2-6 minutes, where the higher content led to the quicker overshoot onset indicating the onset of peroxide-initiated reaction, potentially into long-chain, branched, or crosslinked structures [19], [20].

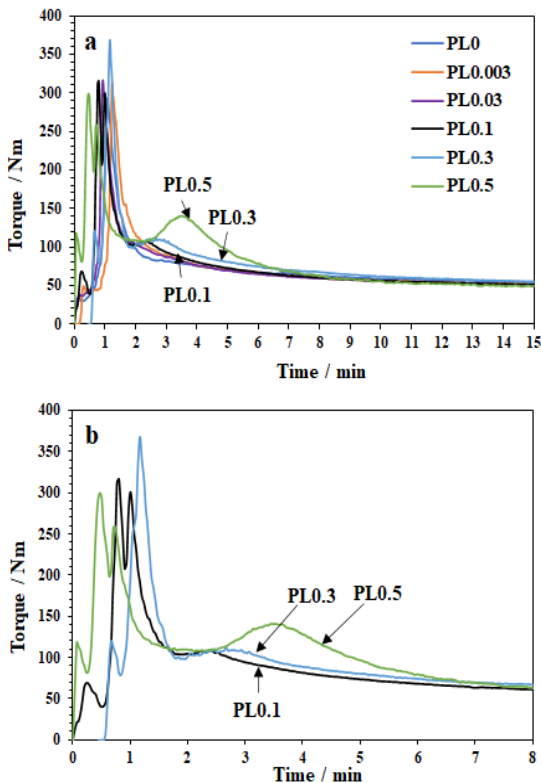


Fig. 5 Torque plastograms during reactive melt-blending of all peroxide-treated PLAs (a) and PLAs treated with 0.1-0.5 wt% peroxide in an enlarged scale (b)

3.2. Rheological Properties and Melt Strength

From the indication of structural changes in the NMR spectra and in the torque plastogram during mixing, the rheological technique, which is more sensitive to structural changes, was investigated in this section. From the dynamic frequency sweep test, the results in the terminal region (low frequencies) are of primary interest as they indicate the properties in the fully-relaxed stage and thus are very sensitive to the difference in molecular structure. The G' indicates the elastic response of the samples, while the G'' and η^* indicate the viscous response. As shown in Figure 6, G' of PLA without the presence of peroxide reached the terminal regime of an entangled linear polymer at an angular frequency below 0.5 rad/s (indicated by the slope of 2.0). With the addition of 0.003 to 0.1 wt% peroxide, the terminal slope was still 2.0, but the graph was shifted to the right, indicating the loss of molecular

weight. It might imply that the role of peroxide at these small concentrations led to chain scission of PLA as proposed by the chain scission mechanism in Figure 2(b). At the higher peroxide content of 0.3 wt%, the G' started to deviate slightly with the terminal slope lower than 2, indicating that the relaxation of the polymer chain was slower due to a more complex structure. The deviation was successively more pronounced at higher percentages of peroxide up to 0.5 wt%, indicating that the structure of PLA deviated from the linear structure into branched or even crosslinked structures. In Figure 7, the reduction of η^* at low peroxide concentrations and its increase at high peroxide contents follows the same trends as G' curves. The η^* curves at 0.3 and 0.5 wt% peroxide also indicated branched structures, which normally possess high η^* at low frequency with a steep decrease in η^* at a higher frequency due to more severe shear thinning.

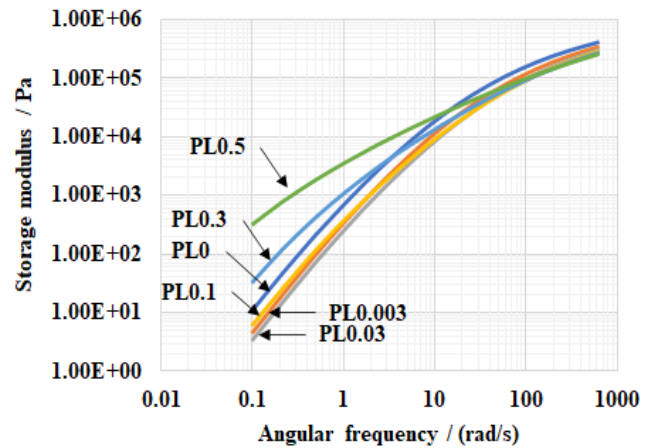


Fig. 6 Storage modulus versus angular frequency of PLA and peroxide-treated PLAs

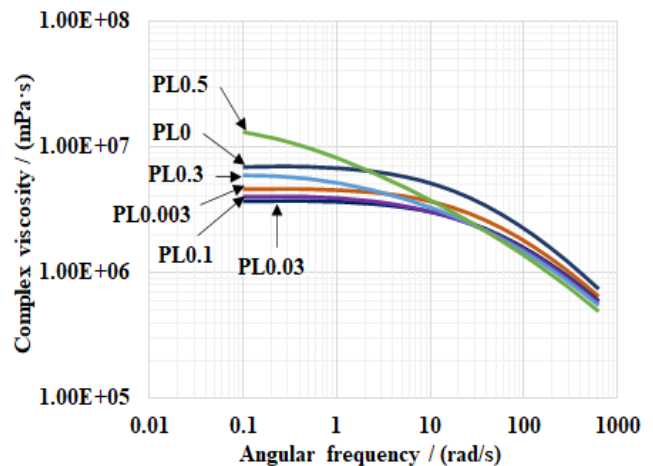


Fig. 7 Complex viscosity versus angular frequency of PLA and peroxide-treated PLAs

The melt strengths of the peroxide-treated PLAs were measured to investigate the changes in extensional properties. As shown in Figure 8, the melt strengths of the peroxide-treated PLAs showed a similar trend to the G' results from the dynamic frequency sweep test in Figure 6. It indicates that the

melt strength is strongly correlated with the elastic modulus of the sample in the molten stage.

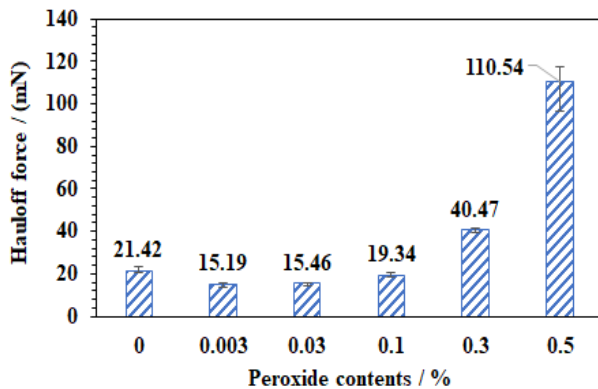


Fig. 8 Melt strengths of PLA and peroxide-treated PLAs

3.3. Processability of Peroxide-Treated PLA Blown Films

In earlier sections, the effect of peroxide treatment was investigated on the changes in molecular structure by linking to rheological properties and the melt strength. This part verifies its effect on the film blowing process by investigating the bubble stability during film blowing. Here, the stability was quantified by the stable bubble chart and the film thickness variation. The two most important process parameters that control the blown film's width and thickness are the blow-up ratio (BUR) and the take-up ratio (TUR). In this study, the TUR of the film blowing process was fixed at 3 different values, which were 1.13, 2.06, and 2.81, while the BUR was increased to the highest stable limit. The stable bubble chart, or so-called the BUR-TUR, was constructed in terms of the highest blow-up ratio (BUR) at each take-up ratio (TUR). The comparative BUR-TUR chart for all samples is shown in Figure 9. As can be seen, the highest BUR tended to increase with TUR at the peroxide content of 0.1% and higher. Since the higher TUR implies a higher extension rate, the increase in the highest BUR indicates that the samples could exhibit an extension hardening behavior. The average values of the highest BURs from all TURs are shown against both the melt strength and the G' values at a low frequency (0.1 rad/s) in Figure 10 to illustrate their strong correlation. In addition, the results also indicate that the peroxide-treated PLAs using the highest peroxide content (0.5 wt%) possessed about 1.2 times higher BUR than the unmodified PLA.

Another parameter that indicates the bubble stability of blown films is the uniformity of film thickness along the machine direction, as indicated by the uniformity index described in section 2.4.6. The results are summarized in Table 2. As can be seen, the uniformity of PLA films tended to be improved at higher peroxide content, where the highest uniformity was observed at the highest peroxide content of 0.5 wt%.

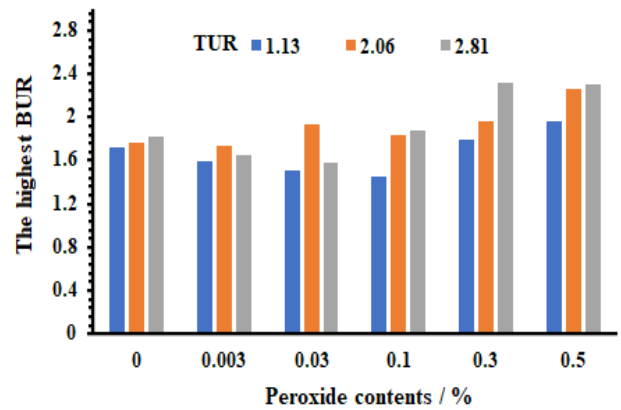


Fig. 9 The highest stable BUR at various TURs for film blowing of PLA and peroxide-treated PLAs

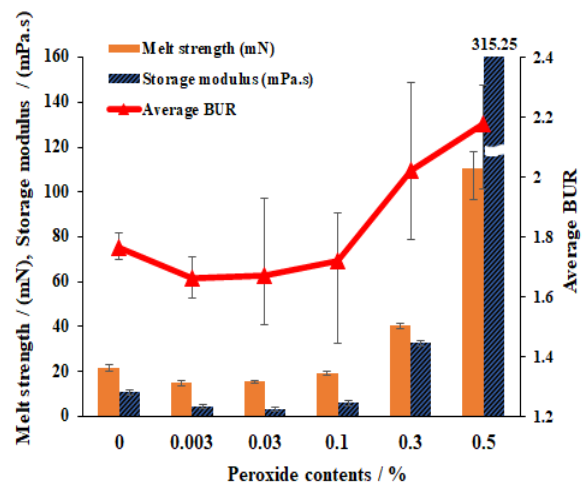


Fig. 10 The average values of the highest BURs from all TURs shown against the melt strength and the G' values at 0.1 rad/s

Table 2 The average film thickness and the uniformity index of PLA and peroxide-treated PLAs blown films

Sample name	Average film thickness / mm	Standard deviation / σ	Uniformity Index
PL0	0.046	0.010	4.805
PL0.003	0.057	0.012	4.898
PL0.03	0.059	0.014	4.142
PL0.1	0.061	0.017	3.589
PL0.3	0.037	0.003	12.440
PL0.5	0.036	0.002	16.358

3.4. Mechanical Properties and Gel Content of Peroxide-Treated PLA Blown Films

It is well-known that PLA films show a brittle fracture with high modulus and very low elongation at break. After reactive blending with peroxide, the changes in tensile properties of PLAs in the machine direction are shown in Figure 11. As can be seen, the modulus and tensile strength slightly increased, while the elongation at break decreased, with increasing peroxide content.

Pursuing quantifying the presence of gel in the peroxide-treated PLA blown film, the insoluble fractions of PLA compounds after being immersed in acetone were reported in terms of gel contents, as shown in Figure 12. As can be seen, the gel contents of PLA and modified PLAs using up to 0.03 wt%

peroxide were comparable. In contrast, the amount of gel was significantly increased when using the highest peroxide content of 0.5 wt%. The presence of visible gels indicated that the number of gels was high enough to cause trouble to the film blowing process. It could lead to premature screen pack blockage or unstable bubbles, especially when running at high TUR. Therefore, the maximum recommended peroxide content for this work would be 0.3 wt%.

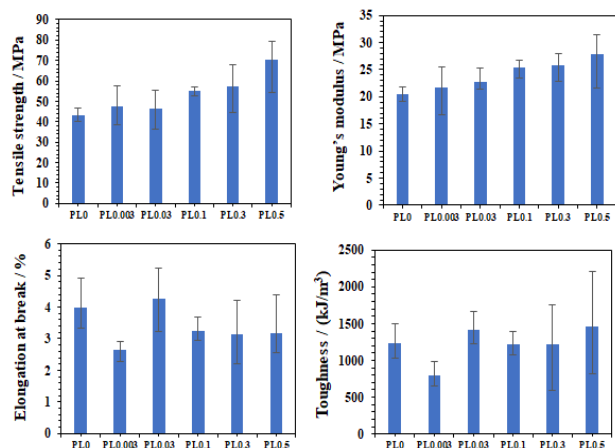


Fig. 11 The tensile properties of PLA and peroxide-treated PLA films

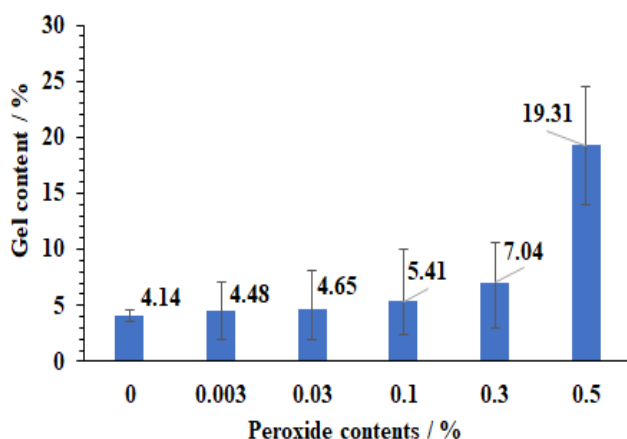


Fig. 12 The gel contents of PLA and peroxide-treated PLA films

4. Conclusion

This study is the first study investigating the effect of peroxide on the film blowing processability of PLA by correlating with the changes in its molecular structures and rheological properties. It was found that a small peroxide content led to lower G' at the terminal regime, indicating the occurrence of chain scission, while a higher content led to an increase in the G' , implying a change into branched or crosslinked structures. Undesirable crosslinked structures were detected at the highest peroxide content (0.5 wt%), as confirmed by the NMR technique and the substantial amount of insoluble gels. It was also found that the rheological parameter G' at the low-frequency regime could be a good indicator for the processability of PLA blown films as it correlated very well with the melt strength, the highest stable BUR, and the thickness uniformity of the film. In this study, even though the

peroxide content of 0.5 wt% could provide the highest film processability, the lower amount of 0.3 wt% was optimal to avoid the presence of gels. Even though peroxide could improve the processability of PLA, the films produced from peroxide-treated PLA tended to be stiffer than those produced from neat PLA, especially when using a higher peroxide content. Further improvement in the film toughness should be carried out by blending with plasticizers or toughening agents.

Acknowledgments

The authors are grateful for the financial support from the Thailand Science Research and Innovation (TSRI) through the Royal Golden Jubilee Ph.D. Program Scholarship (Grant no. PHD/0058/2557) and research funding from the National Research Council and TSRI (Grant no. RDG60T0129). The additional financial support from the research unit in polymer rheology and processing, Thammasat University, is also gratefully acknowledged.

References

- [1] ZHAO X., HU H., WANG X., YU X., ZHOU W., and PENG S. Super tough poly (lactic acid) blends: A comprehensive review. *RSC Advances*, 2020, 10(22): 13316-13368. <https://doi.org/10.1039/D0RA01801E>
- [2] MANGARAJ S., MOHANTY S., SWAIN S., and YADAV A. Development and characterization of commercial biodegradable film from PLA and corn starch for fresh produce packaging. *Journal of Packaging Technology and Research*, 2019, 3(2): 127-140. <https://doi.org/10.1007/s41783-019-00055-y>
- [3] ASHWIN B., ABINAYA B., PRASITH T. P., CHANDRAN S. V., YADAV L. R., VAIRAMANI M., and SELVAMURUGAN N. 3D-poly (lactic acid) scaffolds coated with gelatin and mucic acid for bone tissue engineering. *International journal of biological macromolecules*, 2020, 162: 523-532. <https://doi.org/10.1016/j.ijbiomac.2020.06.157>
- [4] JIANG Y., YAN C., WANG K., SHI D., LIU Z., and YANG M. Super-toughed PLA blown film with enhanced gas barrier property available for packaging and agricultural applications. *Materials*, 2019, 12(10): 1663. <https://doi.org/10.3390/ma12101663>
- [5] KARKHANIS S. S., STARK N. M., SABO R. C., and MATUANA L. M. Blown film extrusion of poly (lactic acid) without melt strength enhancers. *Journal of Applied Polymer Science*, 2017, 134(34): 45212. <https://doi.org/10.1002/app.45212>
- [6] STANDAU T., CASTELLÓN S. M., DELAVOIE A., BONTEN C., and ALTSTÄDT V. Effects of chemical modifications on the rheological and the expansion behavior of polylactide (PLA) in foam extrusion. *e-Polymers*, 2019, 19(1): 297-304. <https://doi.org/10.1515/epoly-2019-0030>
- [7] LAMNAWAR K., MAAZOUZ A., CABRERA G., and AL-ITRY R. Interfacial tension properties in biopolymer blends: From deformed drop retraction method (DDRM) to shear and elongation rheology-application to blown film extrusion. *International Polymer Processing*, 2018, 33(3): 411-424. <https://doi.org/10.3139/217.3614>

- [8] KARKHANIS S. S., & MATUANA L. M. Extrusion blown films of poly (lactic acid) chain-extended with food grade multifunctional epoxies. *Polymer Engineering & Science*, 2019, 59(11): 2211-2219. <https://doi.org/10.1002/pen.25224>
- [9] JIANG Y., YAN C., WANG K., SHI D., LIU Z., and YANG M. Super-toughed PLA blown film with enhanced gas barrier property available for packaging and agricultural applications. *Materials*, 2019, 12(10): 1663. <https://doi.org/10.3390/ma12101663>
- [10] JIANG Y., LI Z., SONG S., SUN S., and LI Q. Highly-modified polylactide transparent blends with better heat-resistance, melt strength, toughness and stiffness balance due to the compatibilization and chain extender effects of methacrylate-co-glycidyl methacrylate copolymer. *Journal of Applied Polymer Science*, 2021, 138(13): 50124. <https://doi.org/10.1002/app.50124>
- [11] GÖTTERMANN S., STANDAU T., WEINMANN S., ALTSTÄDT V., and BONTEN C. Effect of chemical modification on the thermal and rheological properties of polylactide. *Polymer Engineering & Science*, 2017, 57(11): 1242-1251. <https://doi.org/10.1002/pen.24505>
- [12] HWANG S. W., JUNG W. S., and SEO K. H. Preparation Characterization of Modified Poly (Lactic Acid) using dicumyl peroxide and tetraglycidyl diamino diphenyl methane. *Journal of Polymers and the Environment*, 2021. <https://doi.org/10.1007/s10924-021-02174-7>
- [13] JIANG W., GE X., ZHANG B., XING R., and CHANG M. Different influences of two peroxide initiators on structure and properties of poly (lactic acid). *Journal of Vinyl and Additive Technology*, 2020, 26(4): 452-460. <https://doi.org/10.1002/vnl.21760>
- [14] SU S., KOPITZKY R., TOLGA S., and KABASCI S. Polylactide (PLA) and its blends with poly (butylene succinate) (PBS): A brief review. *Polymers*, 2019, 11(7): 1193. <https://doi.org/10.3390/polym11071193>
- [15] YAMOUM C., MAIA J., and MAGARAPHAN R. Rheological and thermal behavior of PLA modified by chemical crosslinking in the presence of ethoxylated bisphenol A dimethacrylates. *Polymers for Advanced Technologies*, 2017, 28(1): 102-112. <https://doi.org/10.1002/pat.3864>
- [16] SRIMALANON P., PRAPAGDEE B., MARKPIN T., and SOMBATSOMPOP N. Effects of DCP as a free radical producer and HPQM as a biocide on the mechanical properties and antibacterial performance of in situ compatibilized PBS/PLA blends. *Polymer Testing*, 2018, 67: 331-341. <https://doi.org/10.1016/j.polymertesting.2018.03.017>
- [17] YUNIARTO K., PURWANTO Y. A., PURWANTO S., WELT B. A., PURWADARIA H. K., and SUNARTI T. C. Infrared and Raman studies on polylactide acid and polyethylene glycol-400 blend. *AIP Conference Proceedings*, 2016, 1725: 020101. <https://doi.org/10.1063/1.4945555>
- [18] ŁOPUSIEWICZ Ł., JEĐRA F., and MIZIELIŃSKA M. New poly (lactic acid) active packaging composite films incorporated with fungal melanin. *Polymers*, 2018, 10(4): 386. <https://doi.org/10.3390/polym10040386>
- [19] LI Z., YE L., ZHAO X., COATES P., CATON-ROSE F., and MARTYN M. High orientation of long chain branched poly (lactic acid) with enhanced blood compatibility and bionic structure. *Journal of Biomedical Materials Research Part A*, 2016, 104(5): 1082-1089. <https://doi.org/10.1002/jbm.a.35640>
- [20] CHANTHOT P., KAEOPHIMMUEANG N., LARPSURIYAKUL P., and PATTAMAPROM C. The effect of dynamic vulcanization systems on the mechanical properties and phase morphology of PLA/NR reactive blends. *Journal of Polymer Research*, 2021, 28(2): 1-12. <https://doi.org/10.1007/s10965-020-02364-2>

参考文献:

- [1] ZHAO X., HU H., WANG X., YU X., ZHOU W., and PENG S. 超级坚韧的聚(乳酸)混合物: 全面审查。英国皇家化学学会进展, 2020, 10(22): 13316-13368. <https://doi.org/10.1039/D0RA01801E>
- [2] MANGARAJ S., MOHANTY S., SWAIN S., 和 YADAV A. 用于新鲜农产品包装的聚乳酸和玉米淀粉商业可生物降解薄膜的开发和表征。包装技术与研究杂志, 2019, 3(2): 127-140. <https://doi.org/10.1007/s41783-019-00055-y>
- [3] ASHWIN B., ABINAYA B., PRASITH T. P., CHANDRAN S. V., YADAV L. R., VAIRAMANI M., 和 SELVAMURUGAN N. 用于骨组织工程的涂有明胶和粘酸的3D聚(乳酸)支架。国际生物大分子杂志, 2020, 162: 523-532. <https://doi.org/10.1016/j.ijbiomac.2020.06.157>
- [4] JIANG Y., YAN C., WANG K., SHI D., LIU Z., 和 YANG M. 具有增强的气体阻隔性的超韧聚乳酸吹膜, 可用于包装和农业应用。材料, 2019, 12(10): 1663. <https://doi.org/10.3390/ma12101663>
- [5] KARKHANIS S. S., STARK N. M., SABO R. C., 和 MATUANA L. M. 不含熔体强度增强剂的聚(乳酸)吹膜挤出。应用高分子科学杂志, 2017, 134(34): 45212. <https://doi.org/10.1002/app.45212>
- [6] STANDAU T., CASTELLÓN S. M., DELAVOIE A., BONTEN C., 和 ALTSTÄDT V. 化学改性对聚丙烯在泡沫挤出中的流变学和膨胀行为的影响。电子聚合物, 2019, 19(1): 297-304. <https://doi.org/10.1515/epoly-2019-0030>
- [7] LAMNAWAR K., MAAZOUZ A., CABRERA G., 和 AL-ITRY R. 生物聚合物共混物中的界面张力特性: 从变形滴回缩方法到剪切和伸长流变学应用到吹膜挤出。国际聚合物加工, 2018, 33(3): 411-424. <https://doi.org/10.3139/217.3614>
- [8] KARKHANIS S. S., 和 MATUANA L. M. 用食品级多功能环氧树脂扩链的聚(乳酸)挤出吹塑薄膜。高分子工程与科学, 2019, 59(11): 2211-2219. <https://doi.org/10.1002/pen.25224>
- [9] JIANG Y., YAN C., WANG K., SHI D., LIU Z., 和 YANG M. 具有增强的气体阻隔性的超韧聚乳酸吹膜, 可用于包装和农业应用。材料, 2019, 12(10): 1663. <https://doi.org/10.3390/ma12101663>
- [10] JIANG Y., LI Z., SONG S., SUN S., 和 LI Q. 由于甲基丙烯酸-共-甲基丙烯酸缩水甘油酯共聚物的增容和扩链作用, 高度改性的聚乳酸透明共混物具有更好的耐热性、熔体强度

- 、韧性和刚度平衡。应用高分子科学杂志, 2021, 138(13): 50124. <https://doi.org/10.1002/app.50124>
- [11] GÖTTERMANN S., STANDAU T., WEINMANN S., ALTSTÄDT V., 和 BONTEN C. 化学改性对聚丙交酯热性能和流变性能的影响。高分子工程与科学, 2017, 57(11): 1242-1251. <https://doi.org/10.1002/pen.24505>
- [12] HWANG S. W., JUNG W. S., 和 SEO K. H. 使用过氧化二枯基和四缩水甘油二氨基二苯基甲烷制备改性聚乳酸的表征。聚合物与环境杂志, 2021. <https://doi.org/10.1007/s10924-021-02174-7>
- [13] JIANG W., GE X., ZHANG B., XING R., 和 CHANG M. 两种过氧化物引发剂对聚乳酸结构和性能的不同影响。乙烯基与添加剂技术杂志, 2020, 26(4): 452-460. <https://doi.org/10.1002/vnl.21760>
- [14] SU S., KOPITZKY R., TOLGA S., 和 KABASCI S. 聚乳酸及其与聚(丁二酸丁二醇酯)的混合物: 简要回顾。聚合物, 2019, 11(7): 1193. <https://doi.org/10.3390/polym11071193>
- [15] YAMOUM C., MAIA J., 和 MAGARAPHAN R. 在乙氧基化双酚一种二甲基丙烯酸酯存在下通过化学交联改性的聚乳酸的流变和热行为。用于先进技术的聚合物, 2017, 28(1): 102-112. <https://doi.org/10.1002/pat.3864>
- [16] SRIMALANON P., PRAPAGDEE B., MARKPIN T., 和 SOMBATSOMPOP N. 过氧化二枯基作为自由基产生剂和 2-羟丙基-3-哌嗪基喹啉羧酸甲基丙烯酸酯作为杀生物剂对原位增容聚丁二酸丁二酯/聚乳酸共混物的机械性能和抗菌性能的影响。聚合物测试, 2018, 67: 331-341. <https://doi.org/10.1016/j.polymeresting.2018.03.017>
- [17] YUNIARTO K., PURWANTO Y. A., PURWANTO S., WELT B. A., PURWADARIA H. K., 和 SUNARTI T. C. 聚乳酸和聚乙二醇400混合物的红外和拉曼研究。美国物理学会会议论文集, 2016, 1725: 020101. <https://doi.org/10.1063/1.4945555>
- [18] ŁOPUSIEWICZ Ł., JĘDRA F., 和 MIZIELIŃSKA M. 新型聚(乳酸)活性包装复合膜与真菌黑色素结合。聚合物, 2018, 10(4): 386. <https://doi.org/10.3390/polym10040386>
- [19] LI Z., YE L., ZHAO X., COATES P., CATON-ROSE F., 和 MARTYN M. 具有增强血液相容性和仿生结构的长链支化聚乳酸的高取向。生物医学材料研究杂志 - 一种部分, 2016, 104(5): 1082-1089. <https://doi.org/10.1002/jbm.a.35640>
- [20] CHANTHOT P., KAEOPHIMMUEANG N., LARPSURIYAKUL P., 和 PATTAMAPROM C. 动态硫化系统对聚乳酸/天然橡胶反应性共混物的机械性能和相形态的影响。高分子研究杂志, 2021, 28(2): 1-12. <https://doi.org/10.1007/s10965-020-02364-2>